Asian Journal of Pharmaceutical Sciences 15 (2020) 728–738

Available online at www.sciencedirect.com

ScienceDirect

journal homepage: www.elsevier.com/locate/AJPS

Original Research Paper

Dynamic micelles with detachable PEGylation at tumoral extracellular pH for enhanced chemotherapy

Guoqing Yan[1], *Panpan Zhang*[1], *Jun Wang*, *Xin Wang*, *Rupei Tang*[*]

Engineering Research Center for Biomedical Materials, School of Life Science, Anhui University, Hefei 230601, China

ARTICLE INFO

Article history:
Received 18 July 2019
Revised 25 September 2019
Accepted 20 November 2019
Available online 3 January 2020

Keywords:
Micelles
Ortho ester
PEGylation
Size transition
Antitumor

ABSTRACT

Although surface PEGylation of nanomedicines can decrease serum protein adsorption *in vivo*, it also blocks uptake by tumor cells. This dilemma could be overcome by employing detachably PEGylated strategy at tumoral extracellular microenvironment to achieve improved cellular uptake while prolonged circulation times. Herein, the amphiphilic graft copolymers with pH-sensitive ortho ester-linked mPEG in side chains and polyurethanes in backbone, can self-assemble into the free and doxorubicin (DOX)-loaded micelles. The pH-sensitive micelles could undergo several characteristics as follows: (i) PEGylated shells for stability in sodium dodecyl sulfonate (SDS) solution; (ii) DePEGylation via degradation of ortho ester linkages at tumoral extracellular pH (6.5) for gradually dynamic size changes and effective release of DOX; and (iii) enhanced cellular uptake and cytotoxicity via positive DOX. Moreover, the dynamic micelles with detachable PEGylation could quickly penetrate the centers of SH-SY5Y multicellular spheroids (MCs) and strongly inhibit tumor growth *in vitro* and *in vivo*, and might be considered as promising and effective drug carriers in tumor therapy.

© 2020 Shenyang Pharmaceutical University. Published by Elsevier B.V.
This is an open access article under the CC BY-NC-ND license.
(http://creativecommons.org/licenses/by-nc-nd/4.0/)

1. Introduction

Polyethylene glycol (PEG) approved by FDA has been widely applied as shielding of nanomedicines to prolong blood circulation times, reduce serum protein adsorption and decrease liver uptake [1–5]. PEGylated polymeric delivery systems such as PEGylated liposomal doxorubicin is highly desirable in clinic cancer treatment, and approve so far minimize toxicity [6–8]. However, they fail to significantly improve the therapeutic efficacy because PEGylation also blocks tumoral cellular uptake, limiting the high-efficiency drug accumulation at tumor sites [9,10]. Therefore, it is an imperious demand to develop a specially PEGylated polymeric delivery system with detachable PEGylation for enhanced chemotherapeutic efficacy [10,11].

To overcome this dilemma, stimuli-triggered strategies have been proposed to construct the polymeric delivery systems with the extracellular DePEGylation upon reaching the targeted tumor [10–13]. Tumor tissues exhibit a distinctly

* Corresponding author. Engineering Research Center for Biomedical Materials, School of Life Science, Anhui University, 111 Jiulong Road, Hefei 230601, China. Tel.: +86 551 63861493.
E-mail address: tangrp99@iccas.ac.cn (R.P. Tang).
[1] These authors contributed equally.
Peer review under responsibility of Shenyang Pharmaceutical University.
https://doi.org/10.1016/j.ajps.2019.11.005
1818-0876/© 2020 Shenyang Pharmaceutical University. Published by Elsevier B.V. This is an open access article under the CC BY-NC-ND license. (http://creativecommons.org/licenses/by-nc-nd/4.0/)

gradient pH distribution from extracellular milieu (pH 6.5–7.0) to intracellular microenvironment (pH 4.5–5.5), so it is a desirable choice to utilize acid-responsive groups to link PEG for tumoral extracellular precise detachable PEGylation [14–16]. However, the most commonly used acid labile chemical groups such as hydrazines, acetals, vinyl ethers and so on, can response to tumoral intracellular pH (4.5–5.5), but not response to tumoral extracellular pH (6.5–7.0) [17–19]. Ortho esters, whose hydrolysis rate might improve 1–4 orders of magnitude compared to above acid labile linkages under mildly acidic conditions, have the potential to response to extracellular pH [20–23]. Moreover, our group has successfully designed a series of ultra-pH-sensitive poly(ortho ester)s-based drug delivery systems with dynamic size transitions at tumoral extracellular pH [24–27]. Thus, an ultra-pH-sensitive polymeric delivery system with extracellular detachable PEGylation may be constructed by optimizing the hydrophilicity of the structures surrounding the ortho ester linkages.

PEG as a hydrophilic polymer, could significantly improve pH sensitivity of ortho esters when chemical linkage together. The design can be implemented via transesterification between hydroxy of PEG and methoxy group of ortho ester monomer as reported previously [28]. Additionally, polyurethanes have been widely developed for medical biomaterials ranging from artificial kidney to drug controlled release, owing to their excellent biocompatibility, adhesiveness and antithrombotic properties, as well as excellent mechanical properties [29]. Moreover, polyurethane structures are easily chemically modified by active groups for hydrophilic/hydrophobic balance and excellently biological functions [30]. In this work, a desirable polymeric drug delivery system with detachable PEGylation could be realized by the tunable combination of polyurethanes in the backbone and orthoester-linked PEG in the side chains, thus achieving ideal chemotherapy efficacy.

2. Materials and methods

2.1. Materials

N, N-dimethylformamide (DMF), toluene, triethylamine (TEA), dimethylsulfoxide (DMSO) and dichloromethane (DCM) were dried from CaH_2 before use. Hexamethylene diisocyanate (HDI), pyridinium p-toluene sulfonate acid (Py-PTSA), dibutyltin dilaurate (DBTDL), N, N-carbonyldiimidazole (CDI), methoxypolyethylene glycol (mPEG) (Mw=550) and 3-(4,5-dimeth-ylthiazol-2-yl)−2,5-diphenylter-razolium bromide (MTT) were purchased from Sigma-Aldrich (China). Doxorubicin hydrochloride (DOX·HCl) was obtained from Meilun Biological Technology Co, Ltd and desalted with TEA before use. 2,2,2-Trifluoro-N-(2–methoxy-1,3-dioxolan-4-ylmethyl) acetamide (TA) and N-(1,3-dihydroxypropan-2-yl)−2,2,2-trifluoroacetamide (NF) were synthesis and purified as described previously [24,28]. Human neuroblastoma cancer cell lines (SH-SY5Y), human liver carcinoma cell line (HepG2) and murine hepatic cancer cell line (H22) were obtained from KeyGEN BioTECH (Nanjing, China). Male ICR mice (18–22 g) were purchased from Animal Center of Anhui Medical University (Hefei, China), and used in the Guide of Experimental Animal Ethics Committee of Anhui University.

2.2. Synthesis of (2-(2-O-mPEG)−1,3-dioxolan-4-yl) methanamine (OEmPEG)

In a nitrogen atmosphere, TA (2.29 g, 10.00 mmol), mPEG (8.25 g, 15.00 mmol), Py-PTSA (0.027 g, 0.06 mmol) and toluene (100 ml) were refluxed together at 115 °C for 8 h. Afterwards, the mixture was concentrated, dissolved in CDM (100 ml), and extracted with saturated NaCl solution in turn. The CDM layer was orderly dehydrated over anhydrous $MgSO_4$, concentrated and stirred in NaOH solution (20 ml, 1.00 mol/l) for 5 h. Finally, the OEmPEG as a white powder (5.22 g, 78.3%) was yielded by extraction with CDM twice, drying over anhydrous $MgSO_4$ and vacuum desiccation. Its structure was determined via ^1H NMR spectrum in $CDCl_3$ using a Bruker AM-400 MHz spectrometer (Bruker Biospin).

2.3. Synthesis of polyurethanes grafting amino ($PU\text{-}g\text{-}NH_2$)

NF (1.34 g, 7.16 mmol), HDI (1.20 g, 7.16 mmol) and a catalytic amount of DBTDL were vigorously stirred together in DMF (7 ml) for 24 h at 25 °C under the protection of nitrogen, and then added dropwise to stirred anhydrous ether. The polyurethanes grafting trifluoro ethyl amide ($PU\text{-}g\text{-}F_3$) were obtained via vacuum drying. Afterwards, $PU\text{-}g\text{-}F_3$ was stirred in 1.00 mol/l of NaOH aqueous solution for 6 h. Finally, $PU\text{-}g\text{-}NH_2$ as a white solid (1.39 g, 75.0%) was obtained via dialysis and lyophilization in turn.

2.4. Synthesis of polyurethanes graft OEmPEG (PU-g-OEmPEGx, x represented the percentage of molar feed between OEmPEG and amino groups in polyurethanes)

The synthesis of PU-g-OEmPEG100 was as follows: OEmPEG-active ester (4.97 g, 7.72 mmol) prepared via reaction between OEmPEG and CDI at the molar ratio of 1 to 1.5, was added to a stirred mixture of $PU\text{-}g\text{-}NH_2$ (1.00 g), TEA (1.56 g, 15.44 mmol), and DMF (30 ml) under nitrogen at 25 °C for 12 h. PU-g-OEmPEG100 as a white solid (3.00 g, 63.8%) was yielded by dialysis (MWCO 3500) against distilled deionized water for 24 h and lyophilization. The other two copolymers were synthesized through the same process. The polymeric structures, grafting degrees and molecular weights were determined by ^1H NMR spectrum, TNBSA assay and gel permeation chromatography (GPC), respectively.

2.5. Micellar formation

The polymeric micelles were formed using a dialysis method. To obtain DOX-loaded micelles (PU-g-OEmPEG-DOX), 40 mg of copolymers and 8 mg of deprotonated DOX were dissolved in 3 ml of DMSO and added dropwise into 20 ml of PBS (pH 7.4) under slowly stirring. Afterwards, the mixture was transferred to dialysis bags (MWCO 3500) for dialysis against PBS (pH 8.0) for 24 h. The free micelles were prepared through the same process as that for DOX-loaded micelles.

2.6. Determination of the critical micelle concentration (CMC)

To measure the concentration at which the copolymers can encapsulate a hydrophobic drug, the CMC studies were done using a fluorescence probe (Nile Red). The copolymers (1.0×10^{-7} to 1 mg/ml) and Nile Red (1×10^{-6} mol/l) were mixed together in PBS at pH 7.4, and a Hitachi spectrofluorophotometer was used to measure the fluorescence signals at a fixed excitation wavelength of 554 nm with an emission spectrum (550–720 nm). The micellar CMC values were confirmed from plots with polymer concentration and maximum absorption wavelength as horizontal and vertical coordinate, respectively.

2.7. Determination of micellar DePEGylation

The DePEGylation of micelles was determined via the hydrolysis rates of ortho ester linkages in side chains. Briefly, the micelles were suspended in PBS (pH 7.4 and 6.5), and immediately lyophilized at preset time points. Afterwards, the lyophilized samples were dissolved in d_6-DMSO and the structural signals were measured via ^{1}H NMR. The peak at 5.85 ppm corresponded to the characteristic proton of ortho esters, and the peaks at 7.99 and 8.25 ppm represented the characteristic protons of hydrolysates of ortho esters. The hydrolysis rates (HR) of ortho esters were calculated as follows:

$$\text{HR}\ (\%) = \frac{(\text{Integrated areas of peaks at 7.99 and 8.25 ppm})}{(\text{Integrated areas of peaks at 5.85, 7.99 and 8.25 ppm})} \times 100\%$$

2.8. Determination of micellar sizes and stability

The micellar average diameters and morphology were determined via Zetasizer dynamic light scattering detector (DLS) and Transmission Electron Microscope (TEM). DLS and/or Scanning Electron Microscope (SEM) were used to evaluate the micellar size changes at pH 7.4 and 6.5 and stability in sodium dodecyl sulfonate (SDS) solution.

2.9. Measurement of micellar drug loading

Micellar drug loading content (DLC) and drug loading efficiency (DLE) were measured and calculated as described before [24].

2.10. In vitro acid-triggered drug release

Micellar DOX release in the PBS (pH 7.4 and 6.5) were studies via a dialysis method. In brief, micelles-DOX were suspended in 1 ml of PBS and dialyzed against 5 ml of the corresponding PBS at 37 °C. At each time points, all release media were sampled and replaced with another 5 ml of PBS. The release amount of DOX was measured via UV–Vis spectroscopy and calculated based on a calibration curve.

2.11. In vitro cytotoxicity and cellular uptake of PU-g-OEmPEG-DOX

HepG2 and SH-SY5Y cells were used to determine micellar cytotoxicity and cellular uptake at pH 7.4 and 6.5 via MTT assay, CLSM and flow cytometry respectively as described before [25].

2.12. Penetration in SH-SY5Y MCs

SH-SY5Y multicellular spheroids (MCs) were successfully cultured as described previously [31,32], and the MCs (200–300 μm) were picked, and co-cultured with various DOX formulations (8 μg/ml) for predetermined time intervals. Afterwards, the culture medium was removed and MCs were thoroughly washed by PBS before observation. Finally, the MCs were imaged and determined by CLSM and Image J. Z-stack, respectively.

2.13. Growth inhibition study in MCs

Briefly, SH-SY5Y MCs (approximately 200–250 μm) were collected and incubated with various DOX formulations (8 μg/ml) for 5 d, and the diameter of each spheroid was observed and taken image using the optical microscope. The volume of MCs was calculated as:

$$V = (\pi \times a \times b)/6$$

Where a and b represent the maximum and the minimum diameter of each MCs, respectively [33].

2.14. In vivo biodistribution

H22 tumor-bearing ICR mice were randomly divided into 4 cohorts (Free DOX and 3 DOX-loaded micelles) of 18 mice each, and drug contents in blood samples and major tissues (heart, liver, kidney, lung, spleen and tumor) of mice at different time point were determined as described [24,25].

2.15. In vivo antitumor effect

The tumor regression study of various DOX formulations were performed using H22 tumor-bearing mice [24,25].

2.16. Statistical analysis

Experimental data are shown as the mean ± standard deviation (SD), and the significance of the data is calculated by SPSS.

3. Results and discussion

3.1. Preparation and characterization of PEGylated polyurethanes and micelleplex systems

As displayed in Fig. 1, ortho ester-linked PEG (OEmPEG) in polymeric side chains was synthesized via transesterification between TA and mPEG using Py-PTSA as a catalyst. Polyurethanes in backbone were synthesized via polyreaction between trifluoroacetyl serinol and hexamethylene diisocyanate at the molar ratio of 1 to 1. After deprotection in the presence of NaOH (1.00 mol/l), PEGylated copolymers were obtained by partially grafting reaction between active OEmPEG and polyurethanes. The structures of intermediate

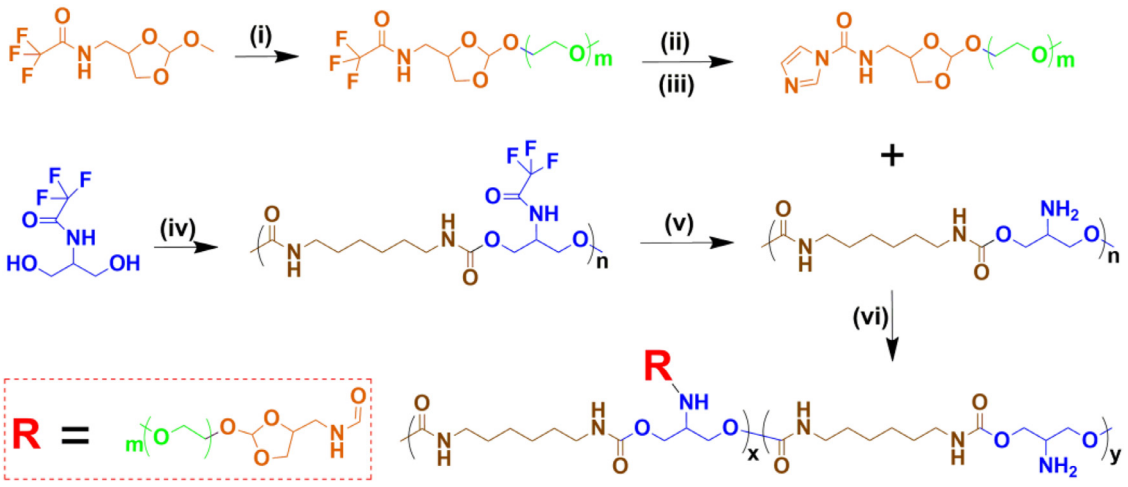

Fig. 1 – Synthetic route of ortho ester-linked PEGylated polyurethanes. Reaction conditions: (i) mPEG/Py-PTSA; (ii) 1.00 mol/l NaOH; (iii) CDI/TEA; (iv) HDI/ DBTDL; (v) 1.00 mol/l NaOH; (vi) TEA.

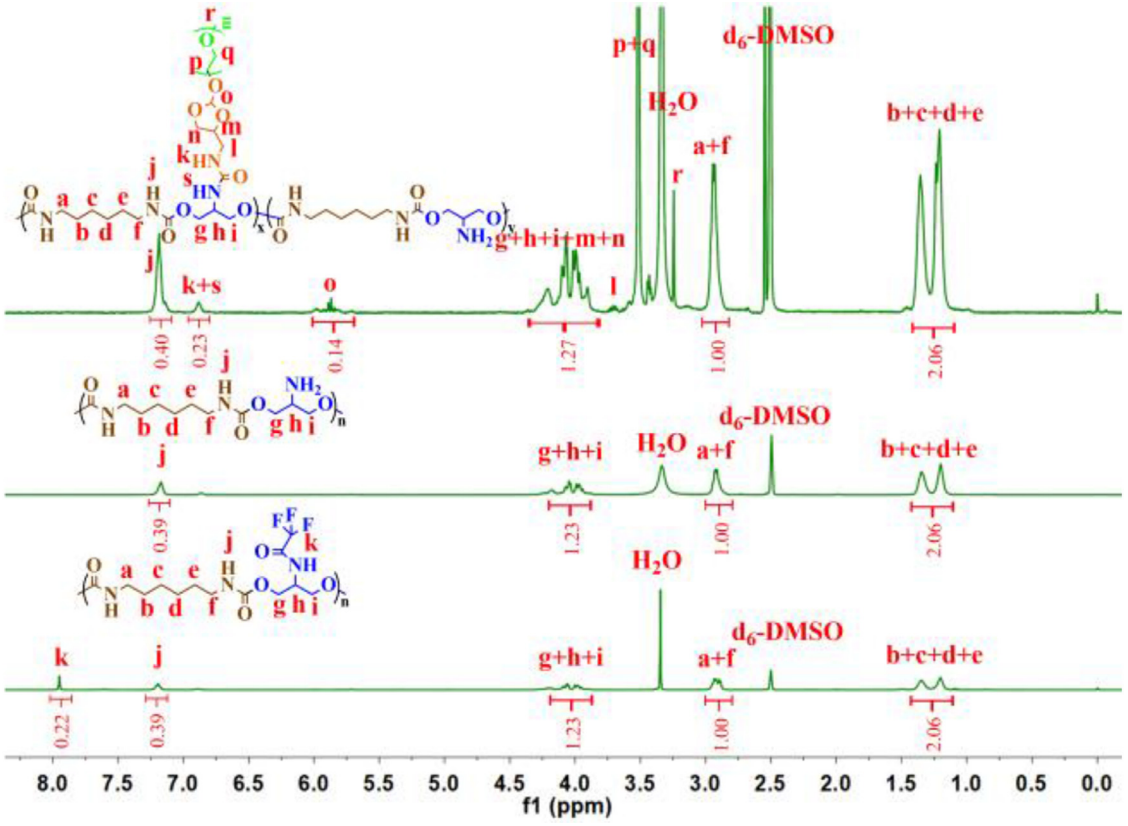

Fig. 2 – ^{1}H NMR spectra of PU-*g*-F_3, PU-*g*-NH_2 and PU-*g*-OEmPEG.

products and PEGylated polyurethanes were confirmed by ^{1}H NMR (Fig. 2), and the degrees of PEGylation in the copolymers were measured to be 55.2%, 74.4% and 96.5% by TNBSA assay [34] and ^{1}H NMR, respectively. The average molecular weights of three PEGylated copolymers were detected to be 2.74×10^4, 3.25×10^4 and 3.91×10^4 g/mol respectively by GPC (Table 1).

Three amphipathic PEGylated polyurethanes could self-assemble to be micelles in a neutral buffer solution. The micellar CMCs were determined to be very lower (0.8–9×10^{-4} mg/ml) using Nile Red as a probe (Fig. 3G), suggesting that three micelles may keep stable when diluted in the blood circulation. The DOX-loaded micelles were also prepared using a solvent exchange method, and the micellar DLC and

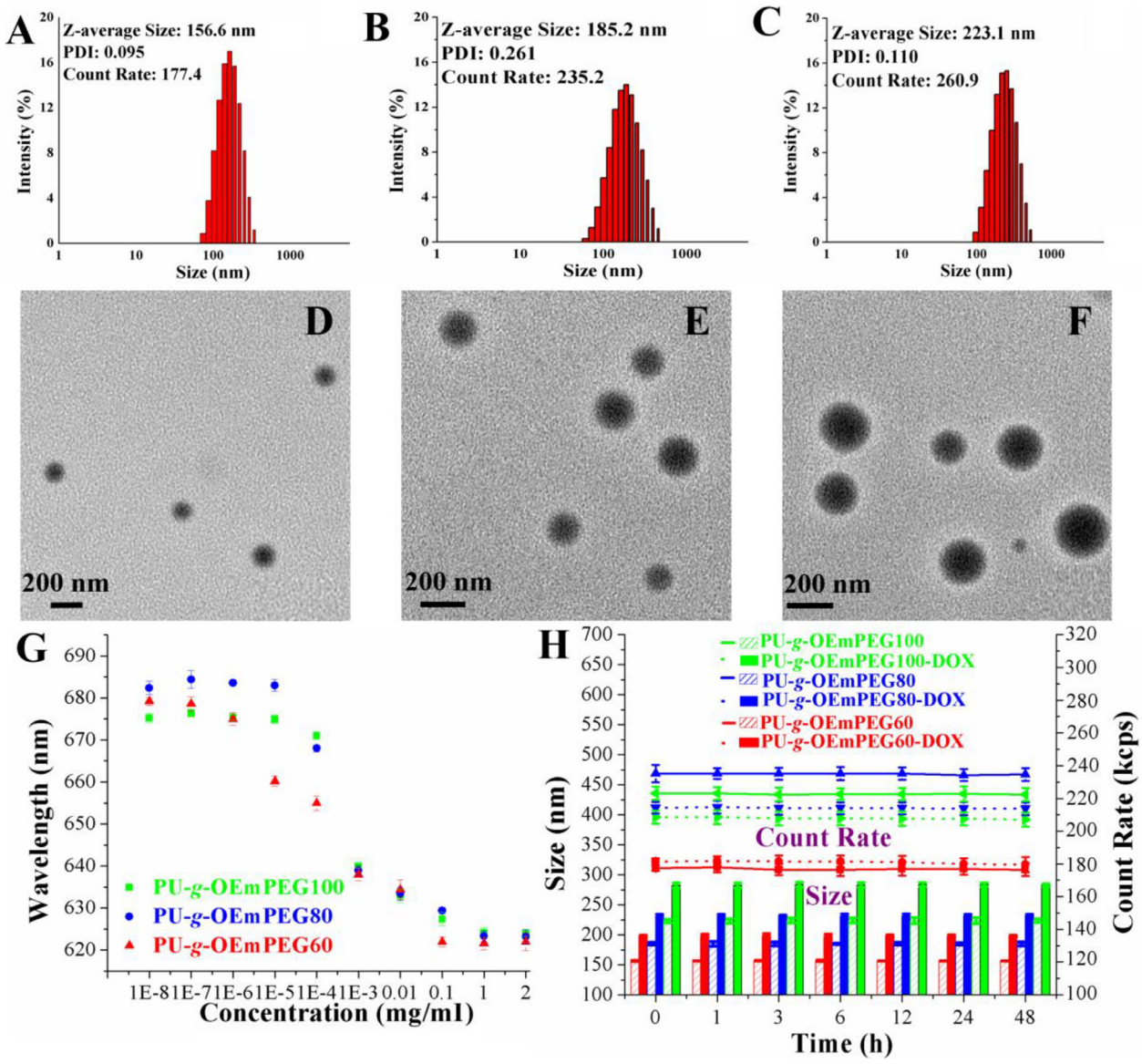

Fig. 3 – Particle size of PU-*g*-OEmPEG60 (A), PU-*g*-OEmPEG80 (B) and PU-*g*-OEmPEG100 micelle (C) measured by DLS; Morphology of PU-*g*-OEmPEG60 (D), PU-*g*-OEmPEG80 (E) and PU-*g*-OEmPEG100 micelle (F) determined by TEM; CMCs (G) and kinetic stabilities in the SDS solution (H).

Table 1 – Yields, molecular weights and grafting degrees of PU-*g*-OEmPEG.

Copolymer	Yield (%)	M_n ($\times 10^4$)	M_w ($\times 10^4$)	PDI	Grafting degree (%)
PU-*g*-OEmPEG100	63.8	3.91	6.15	1.67	96.5
PU-*g*-OEmPEG80	67.4	3.25	5.30	1.74	74.4
PU-*g*-OEmPEG60	70.2	2.74	4.65	1.52	55.2

Table 2 – DLE, DLC and particle sizes of PU-*g*-OEmPEG-DOX.

Material	*DLE* (%)	*DLC* (%)	*Size* (nm)	*PDI*
PU-*g*-OEmPEG100-DOX	55.2	6.7	282.4 ± 2.4	0.141
PU-*g*-OEmPEG80-DOX	62.4	7.9	231.8 ± 1.4	0.123
PU-*g*-OEmPEG60-DOX	71.1	9.4	198.1 ± 3.1	0.121

DLE were measured and calculated to be 6.7%–9.4% and 55.2%–71.1%, respectively (Table 2), at the feeding ratio of 5 to 1 between copolymers and DOX. As seen in Fig. 3A–3C, the average hydrodynamic diameters of PU-*g*-OEmPEG60, PU-*g*-OEmPEG80 and PU-*g*-OEmPEG100 micelle were confirmed to be 156.6, 185.2 and 223.1 nm by DLS, respectively, and were smaller in a drying state observed by TEM (Fig. 3D–3F). In addition, the particle sizes of the DOX-loaded micelles became larger owing to embedding drugs in their hydrophobic cores (Table 2). Interestingly, the hydrophilic/hydrophobic ratio of PU-*g*-OEmPEG impacted on micellar CMCs, particle sizes, and DOX loading. Higher hydrophobicity resulted

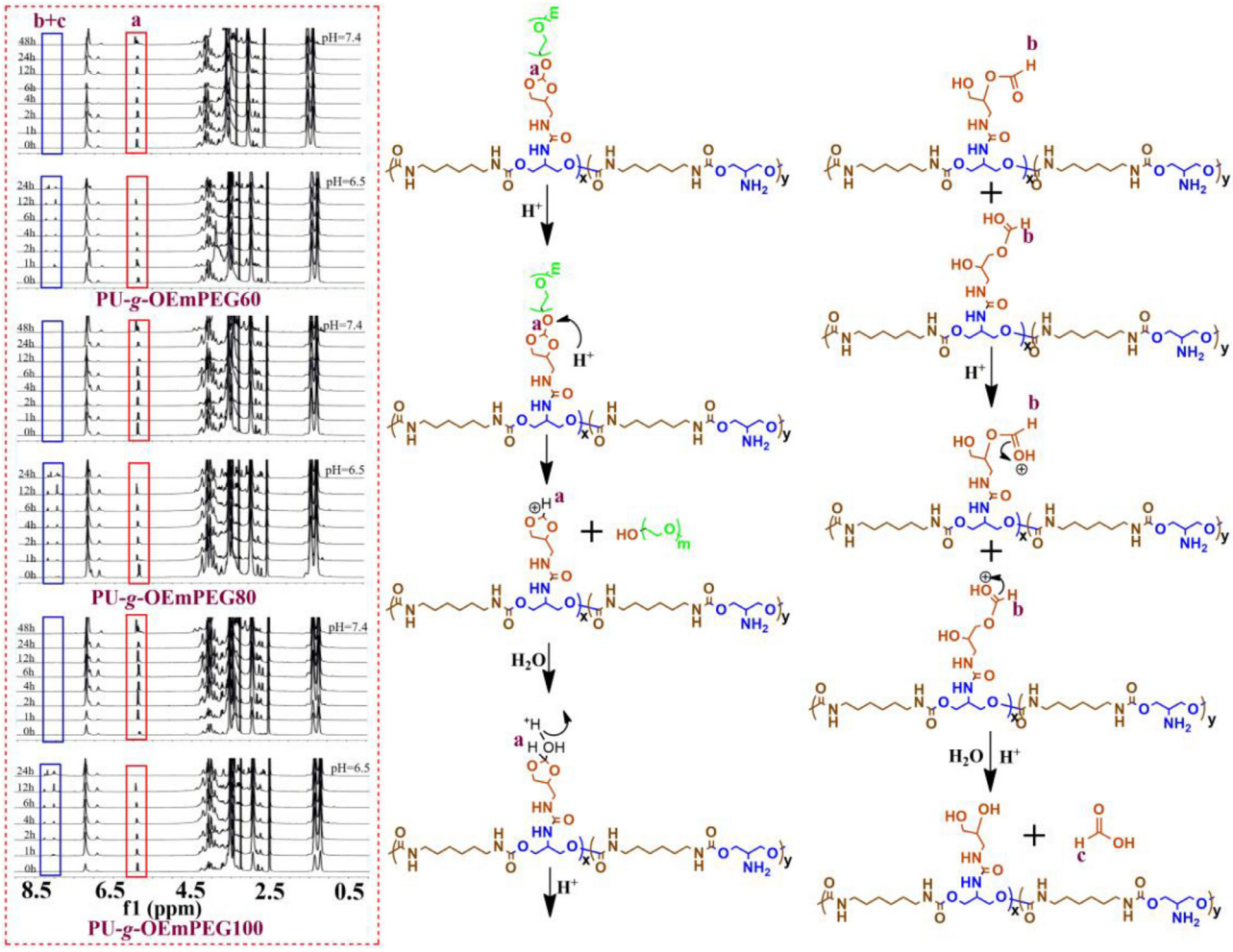

Fig. 4 – Micellar ^{1}H NMR spectra at pH 7.4 and 6.5 following time course and hydrolysis mechanism.

in smaller micellar CMCs and sizes, and higher drug loading. Furthermore, as shown in Fig. 3H, the micellar particle sizes and count rates didn't change in SDS solution for 48 h, suggesting micellar kinetic stability in blood circulation [35].

3.2. *Micellar DePEGyaltion at tumoral extracellular pH*

^{1}H NMR was used to determine the hydrolysis of ortho esters, which represented the micellar DePEGylation. As displayed in Figs. 4 and 5A, three micelles exhibited similar hydrolysis of ortho esters, and ortho esters in side chains were not hydrolyzed in 48 h at pH 7.4, but their hydrolysis was much accelerated at tumoral extracellular pH value (6.5). The degradation of ortho esters reached about 60% in 12 h, and was quickly accomplished in 24 h at pH 6.5. The result revealed that the rapid DePEGylation could be achieved at tumoral extracellular milieu via pH-sensitive OEmPEG in side chains. Moreover, the similar hydrolysis of ortho esters in three micelles may result in similar size changes and drug release. In addition, as shown in Fig. 4, the cleavage of five-membered cyclic ortho esters in side chains yielded formic ether and formate, indicating following a distinct exocyclic mechanism as previously described [20–23].

3.3. *Micellar dynamic size transitions based on detachable DePEGylation*

The detachable DePEGylation in micellar hydrophilic shells had a noticeable impact on particle sizes (Figs. 5B, 5D–5F). The micelles showed similarly dynamic size changes in 24 h at tumor extracellular pH value (6.5). The sizes decreased rapidly in the first 1 h, possibly due to the decrease of hydrophily /hydrophobicity ratio along with the partial DePEGylation, and then gradually increased to above 450 nm in the next 23 h, potentially owing to micellar structural instability with further DePEGylation. It's worth noting that the micellar dynamic size changes at pH 6.5 might be good for tumoral drug accumulation, when initially arriving at tumor sites as small nanoparticles for enhanced penetration and then becoming large nanoparticles within tumors for improved retention [36–38]. Moreover, the dynamic size change may trigger micellar gradual drug release at tumoral extracellular milieu. On the other hand, the micelles

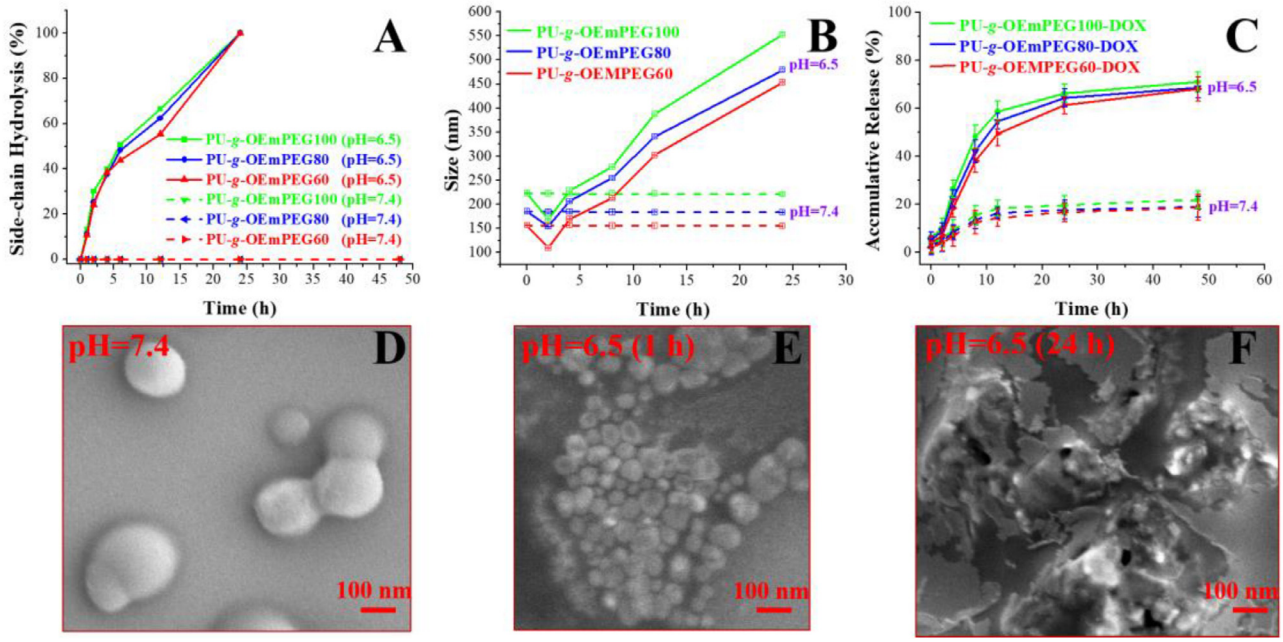

Fig. 5 – Micellar hydrolysis of ortho esters (A), size changes (B) and drug release (C) at pH 7.4 and 6.5 following time course; Morphology and particle size of PU-*g*-OEmPEG60 micelle at pH 7.4 (D), pH 6.5 (1 h) (E) and pH 6.5 (24 h) (F), respectively.

without DePEGylation displayed constant particle sizes at pH 7.4, which was consistent with the results revealed by NMR analysis, suggesting the micellar stability in the circulation.

3.4. *Micellar drug release depending on detachable DePEGylation*

As displayed in Fig. 5C, the micellar DOX release exhibited similarly distinct dependence of detachable DePEGylation. Three DOX-loaded micelles without DePEGylation released only approximately 20% of DOX at pH 7.4 in 24 h. However, the amount of drug release was much increased and reached about 70% for PU-*g*-OEmPEG-DOX at pH 6.5 in 24 h. Such higher amount of drug release was mainly attributed to the micellar gradual swelling with loose structure along with DePEGylation. Moreover, DOX as a positive antitumor drug, can be easily internalized by tumor cells and further enhance cell-killing ability [39].

3.5. *In vitro cytotoxicity and cellular uptake*

To investigate the effect of micellar detachable PEGylation on pharmacological activity, *in vitro* cytotoxicity and cellular uptake of various DOX formulations were compared via SH-SY5Y and HepG2 at pH 7.4 and 6.5 for 24 h, respectively. Meanwhile, the free micelles as negative controls were also exposed to the two types of tumor cells. As seen in Fig. 6A and 6B, the free micelles exhibited no cytotoxicity even at the highest concentration (1000 μg/ml), suggesting their excellent biocompatibility. As displayed in Fig. 6C–6F, PU-*g*-OEmPEG-DOX showed the distinct cytotoxicity along with the increase of drug dosage. Moreover, their cytotoxicity was lower than that of free DOX at pH 7.4, but was similar at pH 6.5. The result implied that the micellar DePEGylation can improve cell-killing ability via extracellular rapid drug release and enhanced cellular internalization of positive DOX revealed by CLSM (Fig. 7A and 7B) and flow cytometry (Fig. 7C–7F), respectively.

3.6. *Penetration in SH-SY5Y MCs*

As displayed in Fig. 8A and 8B, the multicellular spheroids (MCs) prepared from SH-SY5Y cells in the presence of Poly(2-hydroxyethyl methacrylate) as previously described [31,32], can be applied to evaluate the tumor uptake and penetration effects *in vitro*, and the CLSM was used to observe the fluorescence signals of DOX in SH-SY5Y MCs. As shown in Fig. 8C and 8D, free DOX only distributed just within the periphery of MCs in the first 8 h, and penetrated only about 150 μm from the outer layers to the center of MCs after 24 h. While, PU-*g*-OEmPEG-DOX could quickly arise in the center of MCs in the first 8 h, although the fluorescence signals in the center were weak. Moreover, it could be observed that strong fluorescence signals distributed from the periphery toward the center after 12 h, and almost occupied the entire MCs after 24 h. These results suggested that PU-*g*-OEmPEG-DOX could penetrate deeper into MCs than free DOX owing to their dynamic size transitions triggered by DePEGylation [13,36–38].

3.7. *Growth inhibition study in MCs*

Various DOX formulations were incubated with MCs to evaluate the effect of micellar detachable PEGylation on the growth inhibition of MCs. Meanwhile, the culture medium and free micelles as negative controls were also exposed to MCs. As seen in Fig. 9, the controls without cytotoxicity failed

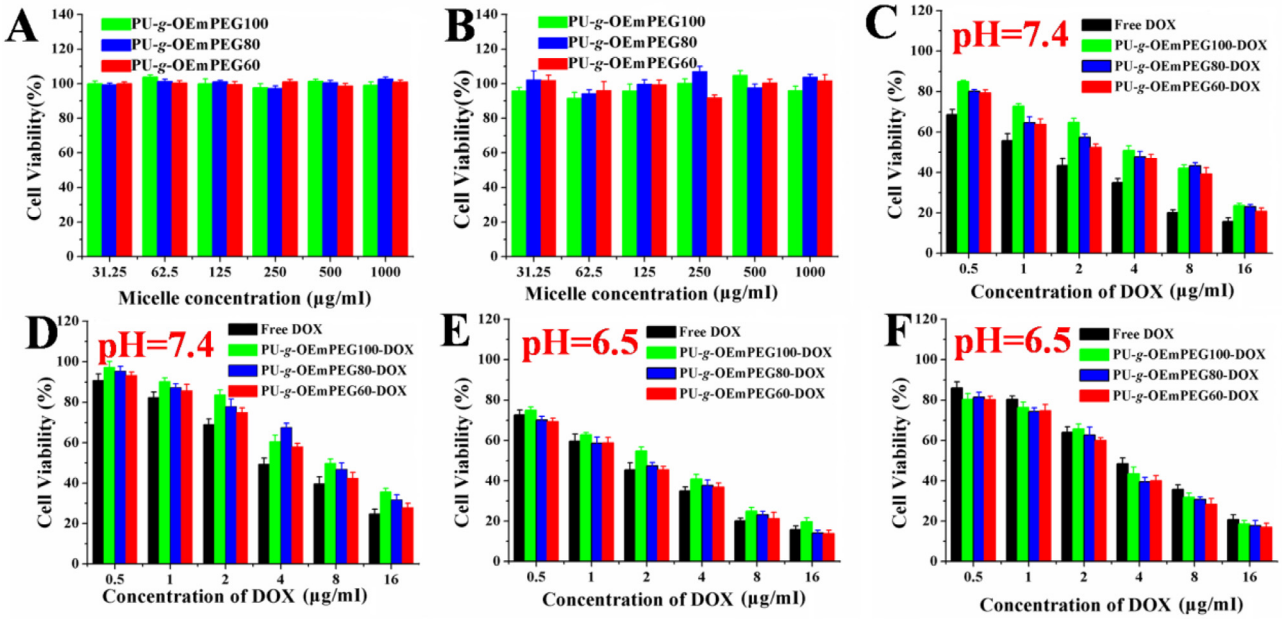

Fig. 6 – *In vitro* cytotoxicity of free micelles, DOX-loaded micelles and free DOX in HepG2 (A), (C) and (E), and SH-SY5Y (B), (D) and (F) at different pH values (7.4 and 6.5).

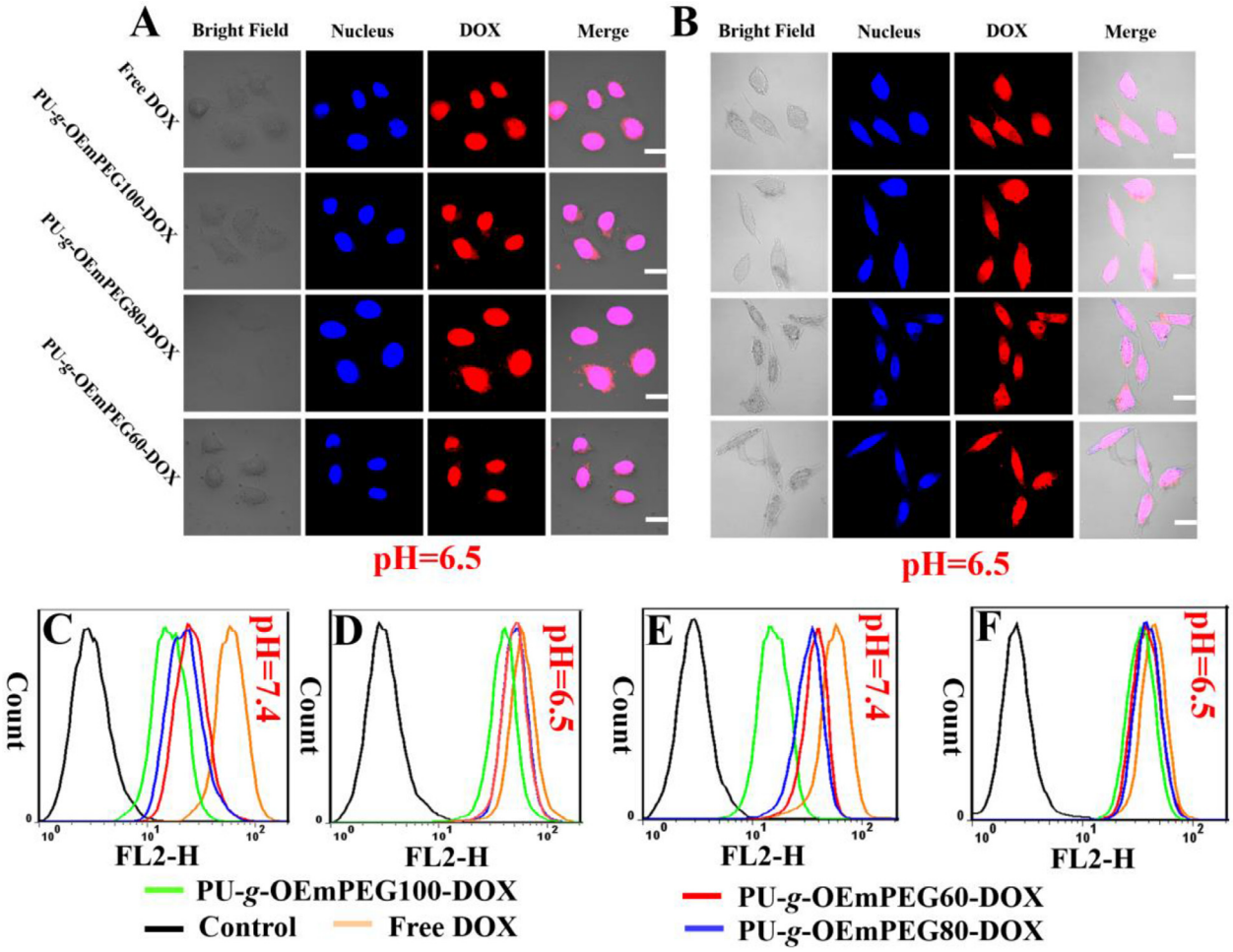

Fig. 7 – Cellular uptake of DOX formulations in HepG2 (A), (C) and (D) and SH-SY5Y (B), (E) and (F) confirmed by CLSM (pH 6.5) and flow cytometry (pH 7.4 and 6.5), respectively; Scale bar = 10 μm.

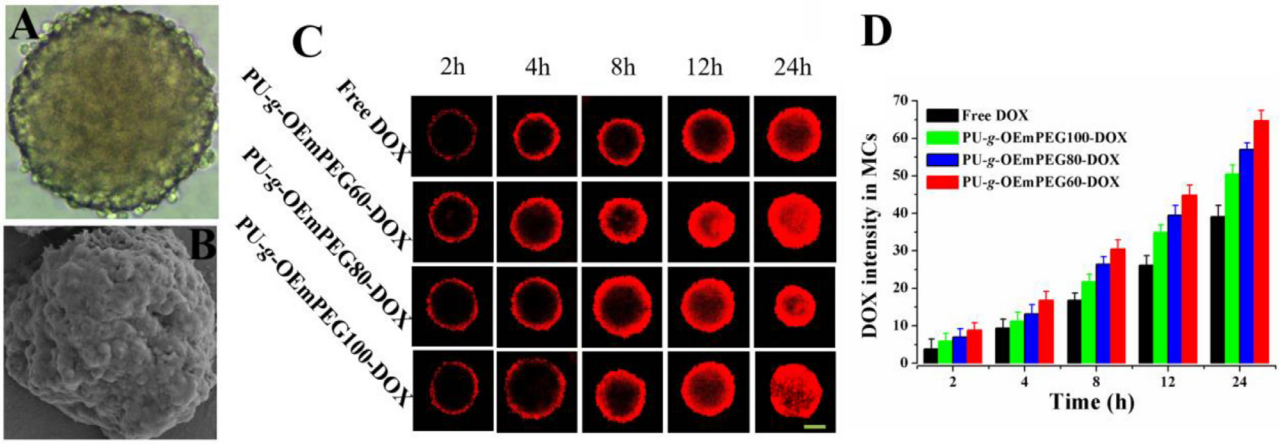

Fig. 8 – SH-SY5Y MCs photographed by inverted microscope (A) and SEM (B), penetration in MCs photographed by CLSM (C), and mean fluorescence intensities of various DOX formulations in MCs (D); Scale bars = 100 μm.

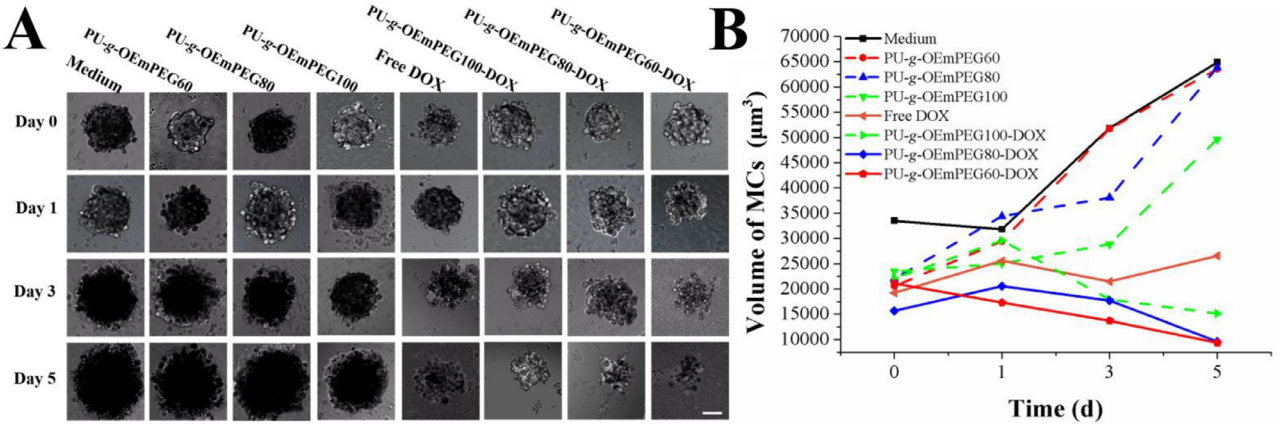

Fig. 9 – Growth inhibition of MCs by formulations: (A) image of MCs following time course and (B) volume of MCs following time course; Scale bars =100 μm.

to stunt tumor growth and the volumes of MCs gradually increased day after day. However, all DOX formulations could efficiently inhibit the growth of MCs and make their volumes smaller day after day. Among them, free DOX limited tumor growth mainly through killing tumoral outer cells, but PU-*g*-OEmPEG-DOX destructed MCs through cytotoxicity from periphery toward center. It is why the outer layers of MCs become loose for free DOX group and the enter MCs become loose for PU-*g*-OEmPEG-DOX group after 3 d. Furthermore, PU-*g*-OEmPEG-DOX turned out to be the best tumor inhibition in all DOX formulations after 5 d. The results agreed well with their stronger tumor penetration of MCs *in vitro*, suggesting that tumoral extracellular DePEGylation, dynamic size transitions and rapid drug release could be beneficial for tumor inhibition [13,36–39].

3.8. *In vivo biodistribution*

To evaluate the effect of micellar detachable PEGylation on *in vivo* drug biodistribution, various DOX formulations were injected into the H22 tumor-bearing mice via i.v. administration. As displayed in Fig. 10, results clearly indicated that DOX concentrations in each tissue varied with different formulations. The amount of DOX in micelles was obviously lower in heart, spleen and lung, but higher in blood than that of free DOX. Moreover, PU-*g*-OEmPEG60-DOX obtained the highest tumoral drug concentration in all formulations, possibly owing to its smaller particle size, stable circulation, enhanced drug penetration and retention via detachable PEGylation and dynamic size change at tumor tissues [13,36–38].

3.9. *Tumor growth inhibition in vivo*

To verify *in vivo* antitumor ability of the micelles with detachable PEGylation, ICR mice bearing tumors derived from H22 cells were used. Treatment began when the tumor volumes were up to 60 mm^3 in all mice. Saline, blank micelle, and DOX formulations (6 mg/kg) were administered via tail vein, respectively, and the injection date was labeled as Day

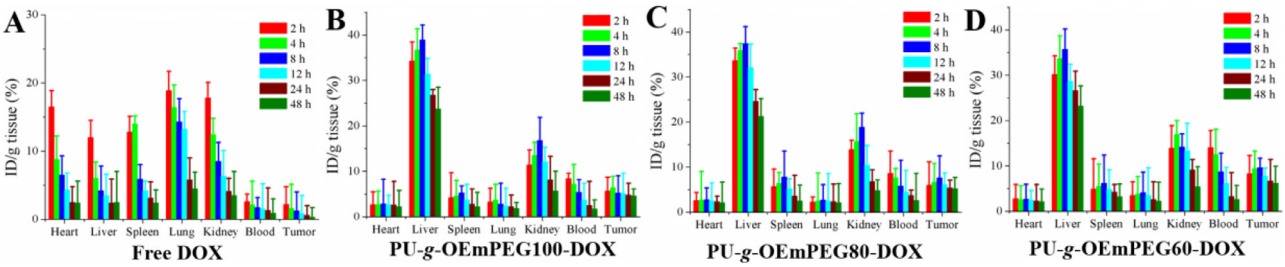

Fig. 10 – *In vivo* biodistribution of DOX in H22 tumor-bearing mice. Data are represented as mean ± SD ($n = 3$).

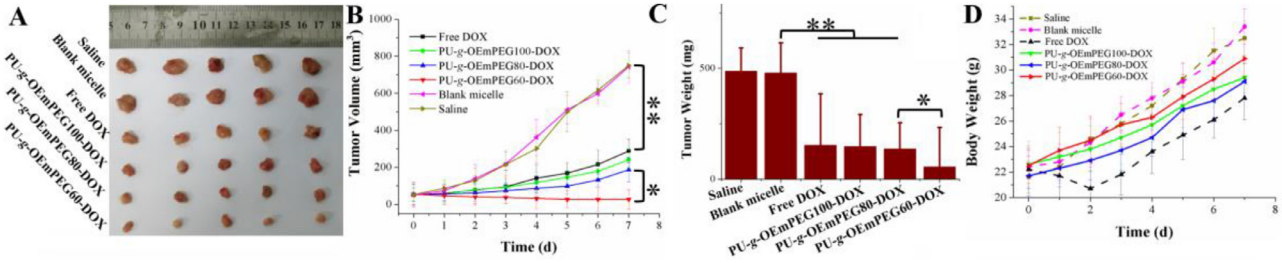

Fig. 11 – Tumor image (A), change trend in tumor volume (B), tumor weight (C) and change trend in body weight (D) of H22 tumor-bearing mice after treatment. (*represents $P < 0.05$ and ** represents $P < 0.01$).

0. The tumor volumes and the body weights of the mice were measured every day, and the tumors were surgically removed, weighed and taken images at the end of the treatment. As seen in Fig. 11A–11C, all DOX formulations obviously restrained tumor growth compared to the control and blank micelle, and PU-*g*-OEmPEG60-DOX achieved the best tumor inhibition and destruction through single intravenous dose. It was probably owing to its efficient tumor accumulation and cytotoxicity to tumor cells. In addition, as shown in Fig. 11D, mice injected with free DOX exhibited a considerable weight loss, suggesting high toxicity of the free drug at this dose. It is possibly attributed to the nonspecific interactions and recognition of free DOX with normal organs, especially heart [40].

4. Conclusion

The detachably PEGylated micelles were successfully constructed and exhibited dynamic size changes and effective drug release along with DePEGylation, via the hydrolysis of ortho ester linkages in side chains at tumoral extracellular pH value (6.5). *In vitro* cytotoxicity and cellular uptake measurements revealed that PU-*g*-OEmPEG-DOX were more easily internalized and had greater toxic effects on tumor cells at tumoral extracellular pH value. Moreover, PU-*g*-OEmPEG-DOX could quickly penetrate the centers of SH-SY5Y multicellular spheroids (MCs) and strongly inhibit tumor growth *in vitro* and *in vivo*. Therefore, the detachably PEGylated micelles with tumoral extracellular dynamic size changes and rapid drug release can serve as promising prototypes with further functionalization in chemotherapy.

Conflicts of interest

The authors report no conflicts of interest. The authors alone are responsible for the content and writing of this article.

Acknowledgments

This work is financially supported by the National Natural Science Foundation of China (No. 51803001, 51603001 and 51503001), the Research Foundation of Education Department of Anhui Province of China (No. KJ2018ZD003 and KJ2018A0006), and the Academic and Technology Introduction Project of Anhui University (AU02303203).

REFERENCES

[1] Hussain Z, Khan S, Imran M, Sohail M, Shah SWA, de Matas M. PEGylation: a promising strategy to overcome challenges to cancer-targeted nanomedicines: a review of challenges to clinical transition and promising resolution. Drug Deliv Transl Res 2019;9:721–34.
[2] Suk JS, Xu Q, Kim N, Hanes J, Ensign LM. PEGylation as a strategy for improving nanoparticle-based drug and gene delivery. Adv Drug Deliv Rev 2016;99:28–51.
[3] Mishra P, Nayak B, Dey RK. PEGylation in anti-cancer therapy: an overview. Asian J Pharm Sci 2016;11(3):337–48.
[4] D'souza AA, Shegokar R. Polyethylene glycol (PEG): a versatile polymer for pharmaceutical applications. Expert Opin Drug Del 2016;13(9):1257–75.

[5] Pelaz B, del Pino P, Maffre P, Hartmann R, Gallego M, Rivera-Fernandez S, et al. Surface functionalization of nanoparticles with polyethylene glycol: effects on protein adsorption and cellular uptake. ACS Nano 2015;9(7):6996–7008.
[6] Bobo D, Robinson KJ, Islam J, Thurecht KJ, Corrie SR. Nanoparticle-based medicines: a review of FDA-approved materials and clinical trials to date. Pharm Res 2016;33(10):2373–87.
[7] Wibroe PP, Ahmadvand D, Oghabian MA, Yaghmur A, Moghimi SM. An integrated assessment of morphology, size, and complement activation of the PEGylated liposomal doxorubicin products Doxil®, Caelyx®, DOXOrubicin, and Sinadoxosome. J Control Release 2016;221:1–8.
[8] Gabizon AA, Patil Y, La-Beck NM. New insights and evolving role of pegylated liposomal doxorubicin in cancer therapy. Drug Resist Update 2016;29:90–106.
[9] Knop K, Hoogenboom R, Fischer D, Schubert US. Poly (ethylene glycol) in drug delivery: pros and cons as well as potential alternatives. Angew Chem Int Ed 2010;49(36):6288–308.
[10] Kong L, Campbell F, Kros A. DePEGylation strategies to increase cancer nanomedicine efficacy. Nanoscale Horiz 2019;4(2):378–87.
[11] Fang Y, Xue J, Gao S, Lu A, Yang D, Jiang H, et al. Cleavable PEGylation: a strategy for overcoming the "PEG dilemma" in efficient drug delivery. Drug Deliv 2017;24(2):22–32.
[12] Chen J, Ding J, Xiao C, Zhuang X, Chen X. Emerging antitumor applications of extracellularly reengineered polymeric nanocarriers. Biomater Sci 2015;3(7):988–1001.
[13] Zhou M, Huang H, Wang D, Lu H, Chen J, Chai Z. Light-triggered PEGylation/DePEGylation of the nanocarriers for enhanced tumor penetration. Nano Lett 2019;19:3671–5.
[14] Zhao C, Deng H, Xu J, Li S, Zhong L, Shao L, et al. "Sheddable" PEG-lipid to balance the contradiction of PEGylation between long circulation and poor uptake. Nanoscale 2016;8(20):10832–42.
[15] Guan X, Guo Z, Wang T, Lin L, Chen J, Tian H. A pH-responsive detachable PEG shielding strategy for gene delivery system in cancer therapy. Biomacromolecules 2017;18(4):1342–9.
[16] Sun C, Liu Y, Du J, Cao Z, Xu C, Wang J. Facile generation of tumor-pH-labile linkage-bridged block copolymers for chemotherapeutic delivery. Angew Chem Int Ed 2016;55(3):1010–14.
[17] Karimi M, Eslami M, Sahandi-Zangabad P, Mirab F, Farajisafiloo N, Shafaei Z, et al. pH-sensitive stimulus-responsive nanocarriers for targeted delivery of therapeutic agents. WIREs Nanomed Nanobiotechnol 2016;8(5):696–716.
[18] Lim EK, Chung BH, Chung SJ. Recent advances in pH-sensitive polymeric nanoparticles for smart drug delivery in cancer therapy. Curr Drug Targets 2018;19(4):300–17.
[19] Liu J, Huang Y, Kumar A, Tan A, Jin S, Mozhi A, et al. pH-sensitive nano-systems for drug delivery in cancer therapy. Biotechnol Adv 2014;32(4):693–710.
[20] Heller J, Barr J. Poly (ortho esters) from concept to reality. Biomacromolecules 2004;5(5):1625–32.
[21] Heller J, Barr J, Ng SY, Abdellauoi KS, Gurny R. Poly(ortho esters): synthesis, characterization, properties and uses. Adv Drug Deliv Rev 2002;54(7):1015–39.
[22] Huang X, Du F, Liang D, Lin S, Li Z. Stereochemical effect of trans/cis isomers on the aqueous solution properties of acid-labile thermoresponsive polymers. Macromolecules 2008;41(14):5433–40.
[23] Cheng J, Ji R, Gao SJ, Du F, Li Z. Facile synthesis of acid-labile polymers with pendent ortho esters. Biomacromolecules 2012;13(1):173–9.
[24] Yan G, Wang J, Hu L, Wang X, Yang G, Fu S, et al. Stepwise targeted drug delivery to liver cancer cells for enhanced therapeutic efficacy by galactose-grafted, ultra-pH-sensitive micelles. Acta Biomater 2017;51:363–73.
[25] Yan G, Wang J, Zhang P, Hu L, Wang X, Yang G, et al. Tunable dynamic fluorinated poly(orthoester)-based drug carriers for greatly enhanced chemotherapeutic efficacy. Polym Chem 2017;8(13):2063–73.
[26] Yan G, Zha Q, Wang J, Wang X, Cheng X, Yao W, et al. Dynamic, ultra-pH-sensitive graft copolymer micelles mediated rapid, complete destruction of 3-D tumor spheroids *in vitro*. Polymer (Guildf) 2017;111:192–203.
[27] Yan G, Wang J, Qin J, Hu L, Zhang P, Wang X, et al. Well-defined poly(ortho ester amides) for potential drug carriers: probing the effect of extra- and intracellular drug release on chemotherapeutic efficacy. Macromol Biosci 2017;17(7):1600503.
[28] Yu M, Zhang L, Wang J, Tang R, Yan G, Cao Z, et al. Acid-labile poly(ortho ester amino alcohols) by ring-opening polymerization for controlled DNA release and improved serum tolerance. Polymer (Guildf) 2016;96:146–55.
[29] Hasirci N, Aksoy EA. Synthesis and modifications of polyurethanes for biomedical purposes. High Perform Polym 2007;19:621–37.
[30] Zdrahala RJ, Zdrahala IJ. Biomedical applications of polyurethanes: a review of past promises, present realities, and a vibrant future. J Biomater Appl 1999;14(1):67–90.
[31] Wang X, Zhen X, Wang J, Zhang J, Wu W, Jiang X. Doxorubicin delivery to 3D multicellular spheroids and tumors based on boronic acid-rich chitosan nanoparticles. Biomaterials 2013;34(19):4667–79.
[32] Wang X, Yang C, Zhang Y, Zhen X, Wu W, Jiang X. Delivery of platinum (IV) drug to subcutaneous tumor and lung metastasis using bradykinin-potentiating peptide-decorated chitosan nanoparticles. Biomaterials 2014;35(24):6439–53.
[33] Wang X, Wei B, Cheng X, Wang J, Tang R. Phenylboronic acid-decorated gelatin nanoparticles for enhanced tumor targeting and penetration. Nanotechnology 2016;27(38):385101.
[34] Sashidhar RB, Capoor AK, Ramana D. Quantitation of epsilon-amino group using amino acids as reference standards by trinitrobenzene sulfonic acid: a simple spectrophotometric method for the estimation of hapten to carrier protein ratio. J Immunol Methods 1994;167:121–7.
[35] Kang N, Perron ME, Prud'homme RE, Zhang Y, Gaucher G, Leroux JC. Stereocomplex block copolymer micelles: core-shell nanostructures with enhanced stability. Nano Lett 2005;5(2):315–19.
[36] Sun Q, Sun X, Ma X, Zhou Z, Jin E, Zhang B, et al. Integration of nanoassembly functions for an effective delivery cascade for cancer drugs. Adv Mater 2014;26(45):7615–21.
[37] Li H, Du J, Du X, Xu C, Sun C, Wang H, et al. Stimuli-responsive clustered nanoparticles for improved tumor penetration and therapeutic efficacy. Proc Natl Acad Sci USA 2016;113(15):4164–9.
[38] Tang R, Ji W, Wang C. Amphiphilic block copolymers bearing ortho ester side-chains: pH-dependent hydrolysis and self-assembly in water. Macromol Biosci 2010;10(2):192–201.
[39] Ko J, Park K, Kim YS, Kim MS, Han JK, Kim K, et al. Tumoral acidic extracellular pH targeting of pH-responsive MPEG-poly(b-amino ester) block copolymer micelles for cancer therapy. J Control Release 2007;123(2):109–15.
[40] Yang Y, Yuan SX, Zhao LH, Wang C, Ni JS, Wang ZG, et al. Ligand-directed stearic acid grafted chitosan micelles to increase therapeutic efficacy in hepatic cancer. Mol Pharm 2015;12(2):644–52.